
Mitigate Position Bias in Large Language Models via Scaling a Single Dimension

**Yijiong Yu^{1†}, Huiqiang Jiang², Xufang Luo², Qianhui Wu², Chin-Yew Lin²,
Dongsheng Li², Yuqing Yang², Yongfeng Huang¹, Lili Qiu²**

¹Tsinghua University, ²Microsoft Corporation

yuyj22@mails.tsinghua.edu.cn, yfhuang@tsinghua.edu.cn

{hjiang, xufluo, qianhuiwu, cyl, dongsli, yuqyang, liliqiu}@microsoft.com

Abstract

Large Language Models (LLMs) are increasingly applied in various real-world scenarios due to their excellent generalization capabilities and robust generative abilities. However, they exhibit position bias, also known as "lost in the middle", a phenomenon that is especially pronounced in long-context scenarios, which indicates the placement of the key information in different positions of a prompt can significantly affect accuracy. This paper first explores the micro-level manifestations of position bias, concluding that attention weights are a micro-level expression of position bias. It further identifies that, in addition to position embeddings, causal attention mask also contributes to position bias by creating position-specific hidden states. Based on these insights, we propose a method to mitigate position bias by scaling this positional hidden states. Experiments on the NaturalQuestions Multi-document QA, KV retrieval, LongBench and timeline reorder tasks, using various models including RoPE models, context window-extended models, and Alibi models, demonstrate the effectiveness and generalizability of our approach. Our method can improve performance by up to 15.2% by modifying just one dimension of hidden states. Our code is available at <https://aka.ms/PositionalHidden>.

1 Introduction

Long-context large language models (LLMs) [1, 2, 3, 4, 5, 6] have recently garnered significant attention within the community, enabling LLMs to handle longer and more complex tasks such as long-context question-answering [7, 8] and repository-level code understanding [9]. However, recent researches [8, 10, 11, 12, 13], indicates that these long-context LLMs struggle to effectively and consistently utilize all the information provided in the context, exhibiting a position bias known as "lost in the middle", which means LLMs tend to ignore information in the middle of the prompt, even though they can utilize the information at the beginning and end of the prompts well. This issue occurs in nearly all LLMs [10, 14, 15], whether they are decoder-only models or encoder-decoder models, powerful models or small LLMs. For example, for the GPT-3.5-Turbo model in the NaturalQuestion multi-document QA task, the performance difference between ground-truth information placed in the middle of the prompt versus at the ends is 22 points with 2.3k tokens prompt [10]. This significantly impacts the practical application of LLMs in real-world scenarios. Studies [16, 17] show that this position bias becomes more severe as the context length increases, hindering the practical application of long-context LLMs.

Previous works have analyzed this issue from the perspectives of data distribution [14, 18, 19] and position embeddings [15, 20]. For example, FILM [19] addresses position bias by constructing data

[†]Work during internship at Microsoft.

with key information distributed in various positions for supervised fine-tuning (SFT). Ms-PoE [15] mitigates position bias by interpolating RoPE [21] using head-wise scaling factors. However, these methods require additional overhead for training or online estimation of scaling coefficients and are currently applicable to only a few models, limiting their generalizability.

To fundamentally understand and alleviate position bias in LLMs, we first explored the micro-level manifestation of position bias in LLMs and observed patterns in the attention weights consistent with position bias. Next, we investigated the underlying causes of attention weight-induced position bias. By respectively modifying position embedding and causal mask, we found that, in addition to position embedding, the causal mask also significantly affects position bias. Further analysis revealed that the causal mask introduces "positional hidden states", which are positively correlated with absolute positions, thereby conveying positional information to LLMs. These positional hidden states appear regardless of what position encoding method is used, including RoPE [21], Alibi [22], and even NoPE [23].

Based on the above findings, we propose a position bias mitigation method named "**scale positional hidden states**". Specifically, we first design a prior-based searching algorithm that quickly identifies which dimensions of hidden states within the model are positional hidden states, using monotonicity, smoothness, and loss on validation sets as indicators. Next, we design an attention modification algorithm that only let the scaled hidden states influence the attention of the last token of the prompt, efficiently implemented using FlashAttention [24].

Extensive experiments on various models, including LLaMA-2 [25], Vicuna [26], Mistral [27], Gemma [28], Qwen [29], and MPT [30], and across different tasks, including Multi-document QA, KV retrieval, LongBench [31] benchmark, and the timeline reorder task [11], demonstrate that our method effectively mitigates position bias by modifying only one dimension of the hidden states of the model, achieving improvements of up to 15.2%. Our method is compatible with various position embeddings, including RoPE [21] and Alibi [22], and shows good generalization.

Our main contributions are as follows:

1. We find that position bias can be reflected in attention patterns.
2. We discover that the causal mask also introduces position bias and generates positional hidden states correlated to absolute positions in the hidden layers.
3. We propose a method for identifying and scaling the positional hidden states to mitigate position bias.

2 Beyond Position Embeddings: Causal Masks Also Contribute to Position Bias in LLMs

This section identifies patterns in attention weights that closely correspond to position bias. Additionally, we discover that, apart from position embeddings, position information in the LLMs can also be generated by the causal mask, which tends to accumulate in a few specific hidden states channels and bears significant responsibility for the emergence of position bias.

2.1 Microscopic Manifestations of Position Bias in Transformers: Attention Weight Patterns

The attention of auto-regressive can be represented by the following equations:

$$\begin{aligned} \mathbf{q} &= \mathcal{P}(W^Q \mathbf{h}(n), n), \quad \mathbf{k} = \mathcal{P}(W^K \mathbf{h}(m), m) \\ \mathbf{a}_{n,m} &= \text{Softmax}\left(\frac{\mathbf{q}\mathbf{k}^T + \text{Mask}}{\sqrt{d}}\right) \end{aligned} \tag{1}$$

where \mathbf{h} is the hidden states, and $\mathbf{h}(n)$ is the hidden state of the n -th token. W^Q, W^K are the weights of the linear layers, \mathcal{P} is the position encoding function like RoPE [21], d is the dimensionality of query and key states, and n and m are the positional order information. Mask is the causal mask.

To explore the micro-level manifestations of position bias in Transformers, we analyzed the attention weights for sentences containing key information, using a KV retrieval task, which requires the model to retrieve the ground-truth value of the given key from a list containing 50 Key-Value pairs (see

Appendix D for details). As shown in Figures 1, in deep layers the model exhibits retrieval-like behavior, focusing on ground-truth information, forming a diagonal pattern observed in Figure 1b. While in other shallow layers, it always focus most attention on the start or end of the prompt, wherever the key information is located, exhibiting vertical lines patterns, as shown in Figure 1a.

In these layers exhibiting retrieval-like behavior, it can be observed that the attention weights for key information (Gold KV) exhibit patterns similar to position bias: when key information is located at the start or end of the prompt, the attention weights focused on it are relatively higher, while in the middle, they are significantly lower. Moreover, we extract the attention to key information (average of layers 15~25) with different context length in Figure 1c, where as the context length grows, the attenuation of attention weights with respect to position becomes more pronounced, reaching almost zero at the middle. More details about this are in Appendix I and D.

Furthermore, in Appendix E, we found artificially adjusting the attention weights to the key information can directly improve the corresponding accuracy. Thus, we claim that position bias is to a large extent caused by the attention weights patterns at the micro level.

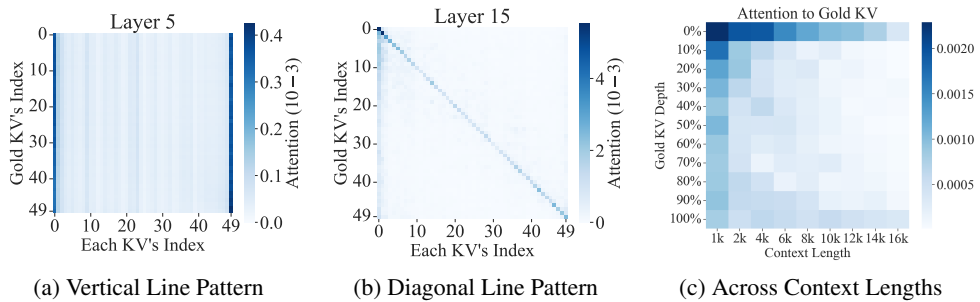


Figure 1: Attention distribution of the ground-truth KV pair to each KV pair across different positions on the KV retrieval task [10] using Mistral-7B [27]. (a) and (b) show the results averaged across all heads of the layer. (c) shows the attention of the ground-truth KV to the ground-truth KV (i.e., diagonal lines from (b)) across different context lengths.

2.2 Causal Mask Also Contributes to Position Bias

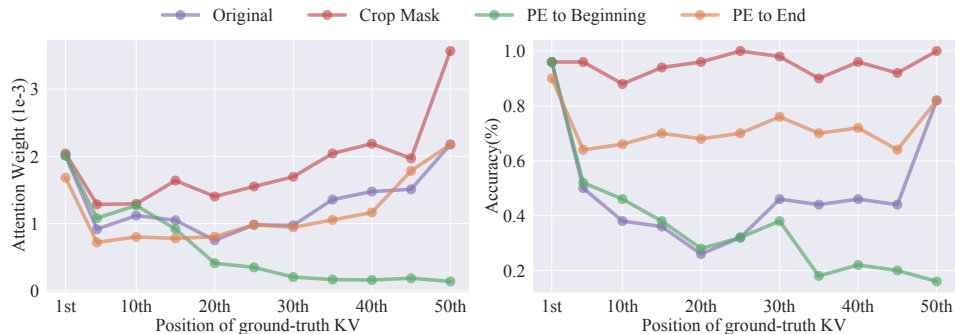


Figure 2: Performance of different methods with the ground-truth KV at different positions in the KV retrieval task [10] using Mistral-7B [27].

Based on Equ.(1), position embedding \mathcal{P} allows LLMs to acquire postional information. However, recent works [23, 32, 33] indicate that, besides position embeddings, the causal mask can also introduce positional information.

Thereby, in this section, we aim to determine whether these two factors affect position bias through modifying different properties of the ground-truth KV pair. Specifically, we introduce the following three baselines: (1) Crop Mask, which modifies the causal mask so that the ground-truth KV pair only sees itself but not the previous tokens. (2) PE to Beginning, which reduces the position IDs

of the ground-truth KV pair to be the same as the first KV pair. (3) PE to End, which increases the position IDs of the ground-truth KV pair to be the same as the last KV pair. More details are provided in Appendix F.

As shown in Figure 2, the original results exhibit a "lost in the middle" pattern not only in accuracy but also in attention weight. Secondly, PE to end has a certain degree of help, but can hardly allow the model's performance to match the accuracy when the ground-truth KV pair is positioned at the start or end of the prompt. Furthermore, PE to Beginning results in a noticeable performance drop as well as attention weight reduction when the gold KV is close to the end. In contrast, modifying the causal mask effectively enhances attention, especially to the latter KVs, and let the performance at the middle be improved to almost on par with the beginning. Based on the above observations, we can conclude that besides position embedding, the causal mask is also an important factor affecting position bias as well as corresponding attention weights. Moreover, solely modifying the position embedding hardly alleviates position bias completely.

2.3 Casual Mask Stores Position Information in Specific Hidden states Channels

Definition 2.1 (Positional Hidden States). *Let $h_k(p)$ denote the k -th dimension of the hidden states across each token's position p . We define positional hidden states h_t as hidden states whose values vary consistently and monotonically with the position sequence. Therefore, their derivative (after curve fitting) should always be positive or negative:*

- $h'_t(p) > 0, \forall p$ or $h'_t(p) < 0, \forall p$

To further analyze how positional information is transmitted in transformers, we define a special type of hidden state that directly reflects absolute positional information with high correlations to position IDs, called positional hidden states, as defined in Definition 2.1. We employ monotonicity rather than correlation as the primary property of positional hidden states, as correlation does not account for the sequential nature of positions. As shown in Figure 3, our experiments reveal that causal LLMs consistently possess such hidden states across most layers (details in Appendix J), even though these models do not have explicit absolute position embeddings, which means the causal mask is a very possible factor that provides absolute positional information. We indeed prove it has major influence on positional hidden states through perturbation experiments on the causal mask and position embedding in Appendix F. So far, combining the conclusion from section 2.2, we can conclude that the causal mask stores positional information in some special hidden states, and further affects attention weights to cause position bias.

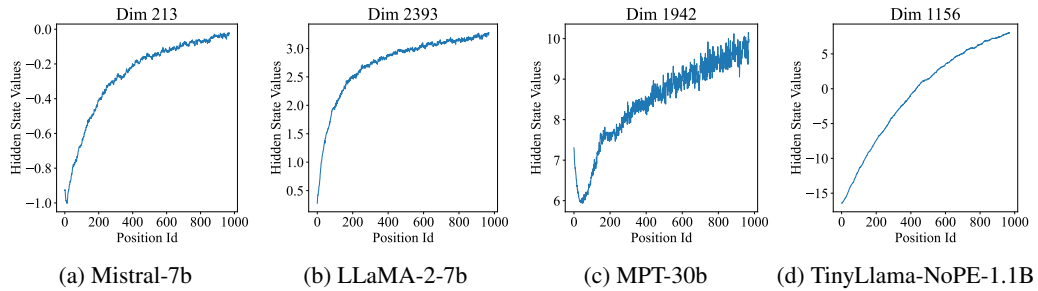


Figure 3: Averaged positional hidden states across all layers in different models.

3 Methodology

Based on the findings in Section 2, although the causal mask profoundly influences position bias, it is not feasible to know the positions of effective information in the prompt in advance, making methods that modify the causal mask difficult to design. Therefore, we propose a method to mitigate position bias by scaling the positional hidden states, as shown in Figure 4. Specifically, it consists of two steps: identifying the positional hidden states h_t and scaling them by the factor s .

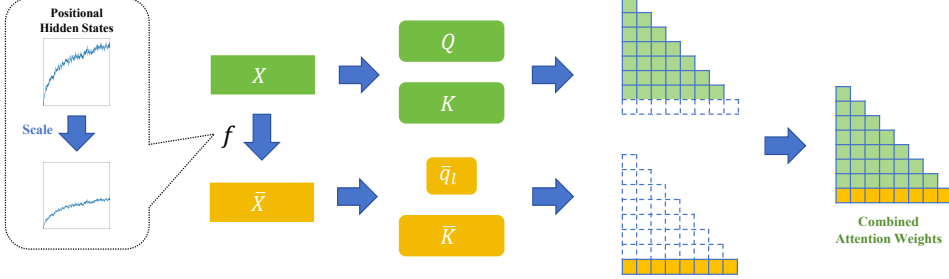


Figure 4: The framework of scaling positional hidden states and modifying attention.

3.1 Problem Formulation

Given a pre-trained LLM θ and a general dataset $\{\mathbf{x}, \mathbf{y}\}$, our objective is to find the optimal positional hidden states h_t and the corresponding scaling factor s to maximally reduce position bias, which can be formulated as follows:

$$\arg \min_{h_t \in \mathcal{H}, s < 1} \mathbb{E} \left[\sum_{i=1}^{|P|} \mathcal{L}(\mathbf{x}, \mathbf{y}, \mathbf{p}_i; F(\theta, h_t, s)) \right] \quad (2)$$

where P represents the set of different positions of the ground-truth information within the prompt \mathbf{x} , $F(\theta, h_t, s)$ denotes the operation of scaling the LLM θ on the t -th dimension of its hidden states by the scaling factor s , and \mathcal{L} denotes the loss for general downstream tasks of the modified model.

3.2 Identifying Positional Hidden States

We have defined positional hidden states in Definition 2.1. However, the original values of hidden states may not strictly satisfy monotonicity. After curve fitting, we can identify dozens or hundreds of dimensions that exhibit various degrees of relevance to positional information. Thus, the first step of our method is to find the dimension that best fits the properties of positional hidden states.

To efficiently search for the positional hidden states from the LLMs' hidden states set, we leverage the characteristics of positional hidden states defined in Section 2.3 and propose a prior-based positional hidden search algorithm. As shown in Algorithm 1, the search process consists of the following two steps: 1) Identify the top- k dimensions ρ in the hidden states that are monotonic in more than ε layers and are as smooth as possible. Here c_t is the number of layers where $h_t(p)$ is monotonic, and g_t is the smooth score of $h_t(p)$. Equ.(3) is the smoothness formula. 2) Use a small validation dataset $\mathcal{D}_{\text{val}} = \{\mathbf{x}, \mathbf{y}\}$ to evaluate the impact of scaling these positional hidden states respectively and select the positional hidden states $h_{\bar{t}}$ that can lead to the minimal loss $\mathcal{L}_{\bar{t}}$.

$$\text{Smooth}(h_t) = \int |h_t''(p)|^2 \quad (3)$$

As for selecting the best scale factor, we take 0.5, 0, -0.5, and -1 to respectively experiment on the validation set, obtain the validation loss, and then select the scaling factor with the lowest loss.

Algorithm 1 Positional Hidden State Search

```

1: Input: LLM  $\theta$ , hidden states  $\mathcal{H}$ , layer number  $L$ , validation set  $\mathcal{D}_{\text{val}}$ , positions set  $P$ , threshold  $\varepsilon$ 
# Identify top-K positional dimensions
2:  $\rho \leftarrow \phi$ 
3: for  $t \leftarrow 1$  to  $|\mathcal{H}|$  do
4:    $c_t \leftarrow 0, g_t \leftarrow 0$ 
5:   for  $l \leftarrow 1$  to  $L$  do
6:     if  $h_t(p) > 0, \forall p$  or  $h_t(p) < 0, \forall p$  then
7:        $c_t \leftarrow c_t + 1, g_t \leftarrow g_t + \text{Smooth}(h_t^l)$ 
8:     end if
9:   end for
10:  if  $c_t > \varepsilon$  then
11:     $\rho \leftarrow \rho \cup \{t\}$ 
12:  end if
13: end for
14:  $\rho \leftarrow \arg \min_K g_t$ 
# Evaluate on the validation dataset
15: for  $t \in \rho$  do
16:    $\mathcal{L}_t \leftarrow 0$ 
17:   for  $p \in P$  do
18:      $\mathcal{L}_t \leftarrow \mathcal{L}_t + \mathcal{L}(\mathbf{x}, \mathbf{y}, p; F(\theta, h_t, s))$ 
19:   end for
20: end for
21:  $\bar{t} \leftarrow \arg \min_{t \in \rho} \mathcal{L}_t$ 
22: return  $\bar{t}$ 

```

3.3 Scaling the Positional Hidden States

To minimize the impact of this modification on the semantics of LLMs, we propose a method scaling the positional hidden states only affecting the last token as shown in Figure 4. Specifically, for the tokens preceding the last token, the attention calculation remains the same as the original. For the last token’s attention computation of a sequence of length l , we obtain the modified query state $\bar{\mathbf{q}}_l$ (of the l -th token, i.e. the last token) and key states $\bar{\mathbf{K}}$ (of all the tokens) by scaling the positional hidden states. That is,

$$\bar{\mathbf{q}}_l = \mathcal{P}(W^Q f(\mathbf{h}(l), p, s), l), \quad \bar{\mathbf{K}} = \mathcal{P}(W^K f(\mathbf{h}, p, s), [1, 2, \dots, l]) \quad (4)$$

Here $f(\mathbf{h}, p, s)$ means the p -th dimension of \mathbf{h} is scaled by the factor s . Therefore, the corresponding attention calculation is as follows:

$$\mathbf{z} = \begin{cases} \text{Softmax}\left(\frac{\mathbf{q}_i \mathbf{K}^\top + \text{Mask}}{\sqrt{d}}\right) \mathbf{V}, & i < l \\ \text{Softmax}\left(\frac{\bar{\mathbf{q}}_l \bar{\mathbf{K}}^\top}{\sqrt{d}}\right) \mathbf{V}, & i = l \end{cases} \quad (5)$$

where \mathbf{z} is the attention output. We use FlashAttention [24] to implement our method with minimal overhead. After obtaining the combined attention weights, the remaining computations are same with the original. As shown in Appendix C.4, our method only causes a slight increase in latency.

4 Experiments

4.1 Setup

Evaluation Tasks and Models We apply our method to a wide range of state-of-the-art open-source LLMs, including: 1) RoPE [34] models: LLaMA-2 (7B, 13B) [25], Mistral-7B [27], Gemma-7B [28], Qwen1.5-7B [29]; 2) Context window extended models: Vicuna (7B, 13B) [26]; 3) Alibi [22] models: MPT-30B [30]. All the models we use are instruction-tuned versions.

And we evaluate the performance across three aspects: 1) Position-bias-related tests on NaturalQuestion multi-document QA [10] and KV retrieval [10] with ground-truth at different positions in the prompt. The NaturalQuestion task includes 20 documents with a prompt length of about 2.3k tokens, while the KV retrieval task includes 140 KV pairs with an average length of about 10k tokens. 2) General long-context benchmark on LongBench [31], including multi-document QA, single-document QA, summarization, few-shot learning, synthetic tasks, and code completion, totaling 16 tasks with an average length of 37k tokens. 3) Position-sensitive tasks on timeline reordering in LoOGLE [11], with an average length of 10k tokens. For prompts that exceed the context windows of LLMs, we follow LongBench’s approach by truncating from the middle and retaining the head and tail of the prompt to fit within the context windows. We use the provided metrics and scripts from the following benchmarks for evaluation.

Implementation Details In this paper, we implement our approach using PyTorch, HuggingFace Transformers, and FlashAttention [24] in an A100 GPU. To ensure stable and reproducible results, we use greedy decoding in all experiments. For the search part, we set the top- k size of positional hidden states to 10 and ε to $L/4$, where L is the number of layers. The validation set is a synthetic KV retrieval dataset consisting of 100 examples, which do not overlap with the test set. The search process takes approximately 10 minutes. For the scaling part, we only modify the intermediate layers of the model to minimize the negative impact on performance. The details of the scaling dimensions, layer ranges, and factors are shown in Table 4. More details are provided in Appendix C.

Baselines We include two training-free positional bias mitigation approaches as our baselines: (i) Original, the original results of LLMs with the ground-truth at different positions in the prompt. (ii) w/ Ms-PoE [15], uses a head-aware position embedding scaling method to mitigate position bias. We follow the paper’s settings and apply scaling coefficients of 1.2 to 1.8 from the 3-rd layer.

Table 1: Performance of different methods with different models on NaturalQuestions (20 docs) [10] and KV retrieval (140 KV pairs) [10] dataset.

Methods	NaturalQuestion							KV Retrieval					
	1st	5th	10th	15th	20th	Avg.	0%	25%	50%	75%	100%	Avg.	
LLaMA-2-7b-chat	32.4	23.8	30.6	31.6	38.2	31.3	77.6	24.6	62.0	35.6	78.0	55.6	
LLaMA-2-7b-chat w/ Ms-PoE	40.8	29.2	33.0	32.8	39.6	35.1	95.0	29.8	21.4	51.8	89.8	57.6	
LLaMA-2-7b-chat w/ Ours	33.6	34.0	40.6	43.0	51.8	40.6	63.6	38.0	82.2	40.6	94.6	63.8	
LLaMA-2-13b-chat	45.2	39.6	40.4	44.2	51.0	44.1	74.2	39.0	70.4	84.4	86.8	71.0	
LLaMA-2-13b-chat w/ Ms-PoE	48.4	41.4	42.4	45.4	52.6	46.0	87.8	28.0	35.4	49.2	83.0	56.7	
LLaMA-2-13b-chat w/ Ours	50.6	43.4	45.0	49.4	58.2	49.3	41.2	17.0	49.6	76.8	84.8	53.9	
Vicuna-7b-v1.5-16k	70.4	54.8	46.8	45.8	47.8	53.1	98.4	0.8	0.2	0.2	0.2	20.0	
Vicuna-7b-v1.5-16k w/ Ms-PoE	67.0	55.2	50.6	46.8	48.2	53.6	97.4	36.8	15.6	5.2	6.6	32.3	
Vicuna-7b-v1.5-16k w/ Ours	63.8	57.6	53.6	51.2	55.6	56.4	95.4	22.0	12.6	5.2	20.4	31.1	
Vicuna-13b-v1.5-16k	67.4	48.2	45.2	45.6	44.4	50.2	95.6	74.2	64.2	58.8	18.2	62.2	
Vicuna-13b-v1.5-16k w/ Ms-PoE	70.0	51.4	46.8	42.8	47.0	51.6	91.8	59.4	71.6	74.4	48.8	69.2	
Vicuna-13b-v1.5-16k w/ Ours	67.4	51.4	47.6	48.8	48.0	52.7	97.2	83.4	80.8	68.8	35.4	73.1	
Mistral-7b-Instruct-v0.2	57.2	55.0	61.2	61.6	62.6	59.5	99.8	93.0	89.0	95.0	94.2	94.2	
Mistral-7b-Instruct-v0.2 w/ Ms-PoE	58.2	60.0	62.6	58.8	62.2	60.4	99.8	95.6	88.4	96.0	95.4	95.0	
Mistral-7b-Instruct-v0.2 w/ Ours	61.2	56.4	63.2	59.8	64.0	60.9	97.6	93.2	90.6	95.6	93.8	94.2	
Gemma-1.1-7b-it	29.6	25.2	28.2	29.6	27.4	28.0	98.6	67.0	62.4	83.4	100.0	82.3	
Gemma-1.1-7b-it w/ Ms-PoE	33.8	29.0	31.6	28.6	28.6	30.3	0.0	0.0	0.0	0.0	0.0	0.0	
Gemma-1.1-7b-it w/ Ours	35.4	31.4	36.0	35.4	35.0	34.6	97.6	95.8	97.6	96.8	99.6	97.5	
Qwen1.5-7b-chat	72.4	53.8	52.2	51.2	54.4	56.8	100.0	97.2	84.6	60.0	56.4	79.6	
Qwen1.5-7b-chat w/ Ms-PoE	67.4	49.8	48.2	47.4	47.0	52.0	3.4	1.4	2.8	2.6	0.6	2.2	
Qwen1.5-7b-chat w/ Ours	67.4	55.2	53.6	56.0	59.4	58.3	97.2	95.6	98.8	76.6	94.4	92.5	
MPT-30b-chat	75.6	49.6	39.0	33.4	39.6	47.4	71.4	34.8	31.6	41.6	74.0	50.7	
MPT-30b-chat w/ Ms-PoE	/	/	/	/	/	/	/	/	/	/	/	/	
MPT-30b-chat w/ Ours	75.0	48.8	41.6	40.6	44.0	50.0	99.0	65.8	48.6	46.6	69.4	65.9	

4.2 Main Results

Tables 1, 2, and 6 present the performance of various methods in different benchmarks. Several observations and conclusions can be drawn: 1) Our method consistently improves overall performance at different positions, with increases of up to 9.3%, 15.2%, and 4.7% in NQ, KV retrieval, and LongBench, respectively, except for LLaMA-2-13B in KV retrieval. Additionally, compared to the SoTA method Ms-PoE, our method shows significant improvements of up to 6.3%, 97.5%, and 14% in NQ, KV retrieval, and LongBench. The poor performance of Ms-PoE in KV retrieval can be attributed to the interpolation causing information loss. 2) Our method effectively enhances LLMs' understanding of information located in the middle and latter parts of the prompt. For key information at the beginning of the prompt, performance is comparable to baselines. Considering only the average performance of the last four positions, our method's improvements over the original increase to 11.3% and 16.8% in NQ and KV retrieval, respectively, and over Ms-PoE increase to 8.7% and 97.5% in NQ and KV retrieval, respectively. 3) Our approach is effective not only for RoPE models but also for context window extended models like Vicuna-16K, which already readjust RoPE [34]. Additionally, our method can be adapted to different position embeddings, such as Alibi [22] models like MPT, resulting in improvements of 2.6%, 15.2%, and 1.2% in NQ, KV retrieval, and LongBench, respectively. 4) Our method demonstrated varying degrees of improvement across different tasks, with the most significant increases being 22.9% in few-shot learning tasks, 8.6% in code tasks, 4% in synthetic tasks, 9.2% in single document QA tasks, and 1.9% in multi-document QA tasks. In summarization tasks, performance was nearly on par with the original results. 5) Our method does not disrupt the necessary position information in LLMs, as detailed in Appendix H.

4.3 Analysis

From Bias to Balance As shown in Table 1, there is an phenomenon that our method mainly benefits when the key information is not at the beginning, but can often decrease performance if the model performs significantly better when the key information is at the beginning. It reveals a possible

Table 2: Performance of different methods with different models on LongBench [31].

Models	SingleDoc	MultiDoc	Synth.	Summ.	FewShot	Code	AVG
LLaMA-2-7b-chat	28.9	29.7	6.6	26.3	10.2	12.2	19.0
LLaMA-2-7b-chat w/ Ms-PoE	29.8	31.7	10.5	26.7	6.4	13.2	19.7
LLaMA-2-7b-chat w/ Ours	29.2	29.3	9.7	25.0	18.9	20.8	22.1
LLaMA-2-13b-chat	21.4	14.6	11.2	26.1	4.7	16.9	15.8
LLaMA-2-13b-chat w/ Ms-PoE	20.8	15.4	12.7	27.3	3.1	15.7	15.8
LLaMA-2-13b-chat w/ Ours	30.6	9.6	10.8	25.7	27.6	18.7	20.5
Vicuna-7b-v1.5-16k	30.2	21.6	7.2	26.7	9.4	21.2	19.4
Vicuna-7b-v1.5-16k w/ Ms-PoE	32.3	24.2	8.3	28.0	9.8	22.2	20.8
Vicuna-7b-v1.5-16k w/ Ours	27.1	22.1	11.2	26.1	16.7	20.2	20.6
Vicuna-13b-v1.5-16k	31.1	33.8	21.2	26.2	21.6	23.8	26.3
Vicuna-13b-v1.5-16k w/ Ms-PoE	34.5	33.1	16.0	27.5	21.0	25.0	26.2
Vicuna-13b-v1.5-16k w/ Ours	30.1	35.1	25.0	25.8	27.0	24.7	27.9
Mistral-7b-Instruct-v0.2	37.8	28.5	49.7	28.8	49.9	44.0	39.8
Mistral-7b-Instruct-v0.2 w/ Ms-PoE	41.7	22.2	38.4	24.9	14.0	19.5	26.8
Mistral-7b-Instruct-v0.2 w/ Ours	38.4	30.4	49.8	29.4	51.4	45.3	40.8
Gemma-1.1-7b-it	39.4	23.2	32.2	24.2	14.4	19.8	25.5
Gemma-1.1-7b-it w/ Ms-PoE	41.7	22.2	38.4	24.9	14.0	19.5	26.8
Gemma-1.1-7b-it w/ Ours	39.0	23.0	35.5	24.5	14.9	19.3	25.7
Qwen1.5-7b-chat	46.4	39.5	38.4	22.3	39.9	44.6	38.5
Qwen1.5-7b-chat w/ Ms-PoE	42.0	41.5	30.3	25.7	43.2	41.4	37.4
Qwen1.5-7b-chat w/ Ours	45.8	38.8	38.5	22.1	40.0	48.1	38.9
MPT-30b-chat	27.9	21.9	7.5	25.7	18.8	16.7	19.7
MPT-30b-chat w/ Ms-PoE	/	/	/	/	/	/	/
MPT-30b-chat w/ Ours	29.4	19.5	6.7	25.8	23.0	21.2	20.9

fact that the positional hidden may be an important factor causing the model to miss the rear parts of the context while focus too much to the beginning parts. Therefore, scaling such dimension can shift the model’s attention from being too focused at the beginning to a more balanced distribution. We validated the above points by testing different scale factors, as shown in Figure 5.

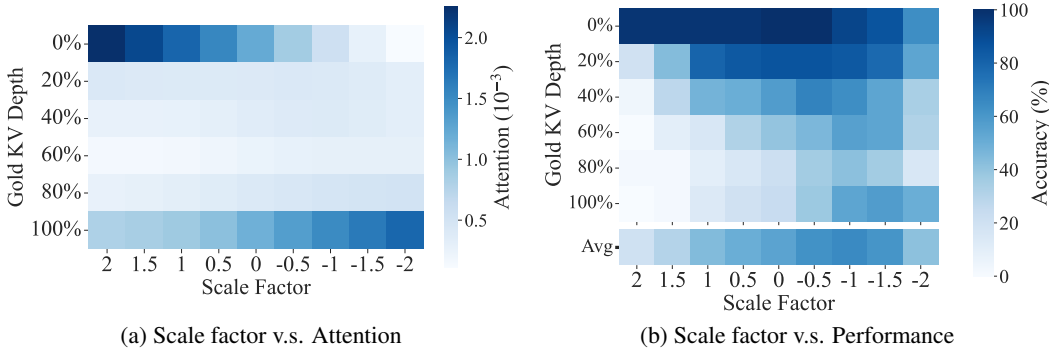


Figure 5: Attention distribution and performance when scaling dimension 2393 of Vicuna-7b-v1.5-16k with different scale factors on KV retrieval [10] of 100 KV pairs.

Scale Factor The scaling factor directly controls the degree and direction of the impact of position hidden states on position bias. As shown in Figure 5, when the scaling factor is positive, the model exhibits a clear bias towards focusing more on the beginning, while when negative, this bias shifts to focusing more on the end. The factor between 0.5 and -1 leads attention to the most balanced distribution, meanwhile, the improvement in accuracy also reaches its peak. This result proves that the positional hidden states we scaled can indeed influence the bias of LLMs towards focusing excessively on the beginning. By adjusting the coefficients appropriately, this bias can be effectively mitigated.

Table 3: Average performance of different ground-truth positions using different methods on NaturalQuestions multi-document QA dataset (20 docs) [10].

Method	LLaMA-2-7b	Vicuna-13b	Gemma-7b	Mistral-7b	Qwen1.5-7b
Original	31.3	50.2	28.0	59.5	56.8
Ours	40.6	52.7	34.6	60.9	58.3
w/o monotonicity	40.6	51.8	34.6	60.9	58.3
w/o smoothness	40.6	52.7	27.8	60.9	58.3
w/o validation set	30.1	51.8	26.5	60.9	58.3
w/ scale 2 dimensions	37.2	50.8	31.7	60.1	57.2
w/ modify last 16 tokens	41.6	51.5	34.6	59.7	58.1
w/ modify all tokens	44.0	50.8	31.7	59.5	57.4

Ablation Study To evaluate the contributions of different components in our method, we introduce the following sets for the ablation study: (1) Ours w/o monotonicity, w/o smoothness, and w/o validation set, which adjust the search algorithm by not considering these three indicators, respectively (details in Appendix C.2). (2) Ours w/ scale 2 dimensions, which modifies the top-2 positional hidden states simultaneously. (3) Ours w/ modify last 16 tokens and w/ modify all tokens, which adjust the range of tokens affected by the scaling operation in Equ.(5).

Table 3 shows the ablation results. It can be seen that without filtering by monotonicity or smoothness, performance may decline, and removing the validation set results in more decline in model performance. When the range of tokens or dimensions affected by scaling is expanded, most models experience varying degrees of performance loss. Considering these factors, we choose to modify only the last token and the top-1 positional dimension to achieve the best performance.

5 Related Works

Long-Context LLMs Recent research has focused on expanding the context window size of LLMs. The main approaches include: 1) Staged pre-training [35, 36]: Gradually increasing the context window size during training. 2) Modifying or interpolating position embeddings [22, 34, 37, 38]. 3) Utilizing external memory modules for context storage [39, 40]. 4) Expanding computations across multiple devices in a distributed manner [41]. While these methods address context window expansion, their impact on positional bias in downstream tasks has yet to be discussed.

Addressing Position Bias Although LLMs incorporate explicit positional information through methods like RoPE [21] or Alibi [22], studies such as [10, 16] have found that LLMs exhibit varying degrees of position bias, referred to as "lost in the middle." Recent works aimed to mitigate this issue and improve LLM performance in long-context scenarios can be categorized as follows: 1) RoPE-based methods: These approaches modify the RoPE computation process to alleviate long-distance information decay, including Attention Bucket [20], which uses an ensemble of multiple RoPE bases to mitigate position bias, and Ms-PoE [15], which dynamically interpolates with a small coefficient for different heads. 2) SFT-based methods [14, 18, 19]: These methods construct data with more diverse key information distributions or employ system2think SFT tasks to mitigate position bias. They require further training of the model. 3) Attention mask-based methods [42]: These methods modify attention mechanisms, including Attention Transition [43], which redirects attention to significant parts of the context and Stable Mask [44], which introduces pseudo attention into the causal mask, ensuring stable attention distribution when facing lengthy texts. 4) Prompt-based methods [45, 46]: These methods introduce an external module to reorder or compress information in the prompt, thereby mitigating position bias.

6 Conclusion

This paper proposes a method for scaling positional hidden states to mitigate position bias issue in LLMs. Specifically, the study first confirms that attention weights manifest position bias within transformers. Additionally, experiments demonstrate that, besides position embeddings, the causal mask also contributes to position bias, which is transmitted to other modules through the hidden

states containing absolute positional information, termed as positional hidden states. Based on this, we introduce a prior-based positional hidden search algorithm and mitigate the model’s position bias by scaling the positional hidden states searched. Testing eight open-source models with different position embeddings on tasks such as NaturalQuestions Multi-document QA, KV Retrieval, and LongBench, the results show that our method effectively reduces position bias and improves model performance.

References

- [1] Gradient. Llama-3 8b instruct gradient 4194k (v0.1), 2024.
- [2] Machel Reid, Nikolay Savinov, Denis Teplyashin, Dmitry Lepikhin, Timothy Lillicrap, Jean-baptiste Alayrac, Radu Soricut, Angeliki Lazaridou, Orhan Firat, Julian Schrittwieser, et al. Gemini 1.5: Unlocking multimodal understanding across millions of tokens of context. *ArXiv preprint*, abs/2403.05530, 2024.
- [3] Hao Liu, Wilson Yan, Matei Zaharia, and Pieter Abbeel. World model on million-length video and language with ringattention. *ArXiv preprint*, abs/2402.08268, 2024.
- [4] Alex Young, Bei Chen, Chao Li, Chengan Huang, Ge Zhang, Guanwei Zhang, Heng Li, Jiangcheng Zhu, Jianqun Chen, Jing Chang, et al. Yi: Open foundation models by 01. ai. *ArXiv preprint*, abs/2403.04652, 2024.
- [5] Marah Abdin, Sam Ade Jacobs, Ammar Ahmad Awan, Jyoti Aneja, Ahmed Awadallah, Hany Awadalla, Nguyen Bach, Amit Bahree, Arash Bakhtiari, Harkirat Behl, Alon Benhaim, Misha Bilenko, Johan BJORCK, Sébastien Bubeck, Martin Cai, Caio César Teodoro Mendes, Weizhu Chen, Vishrav Chaudhary, Parul Chopra, Allie Del Giorno, Gustavo de Rosa, Matthew Dixon, Ronen Eldan, Dan Iter, Amit Garg, Abhishek Goswami, Suriya Gunasekar, Emman Haider, Junheng Hao, Russell J. Hewett, Jamie Huynh, Mojan Javaheripi, Xin Jin, Piero Kauffmann, Nikos Karampatziakis, Dongwoo Kim, Mahoud Khademi, Lev Kurilenko, James R. Lee, Yin Tat Lee, Yuanzhi Li, Chen Liang, Weishung Liu, Eric Lin, Zeqi Lin, Piyush Madan, Arindam Mitra, Hardik Modi, Anh Nguyen, Brandon Norick, Barun Patra, Daniel Perez-Becker, Thomas Portet, Reid Pryzant, Heyang Qin, Marko Radmilac, Corby Rosset, Sambudha Roy, Olatunji Ruwase, Olli Saarikivi, Amin Saied, Adil Salim, Michael Santacroce, Shital Shah, Ning Shang, Hiteshi Sharma, Xia Song, Masahiro Tanaka, Xin Wang, Rachel Ward, Guanhua Wang, Philipp Witte, Michael Wyatt, Can Xu, Jiahang Xu, Sonali Yadav, Fan Yang, Ziyi Yang, Donghan Yu, Chengruidong Zhang, Cyril Zhang, Jianwen Zhang, Li Lyra Zhang, Yi Zhang, Yue Zhang, Yunan Zhang, and Xiren Zhou. Phi-3 technical report: A highly capable language model locally on your phone, 2024.
- [6] DeepSeek-AI. Deepseek-v2: A strong, economical, and efficient mixture-of-experts language model, 2024.
- [7] Avi Caciularu, Matthew E Peters, Jacob Goldberger, Ido Dagan, and Arman Cohan. Peek across: Improving multi-document modeling via cross-document question-answering. pages 1970–1989, 2023.
- [8] Tianle Li, Ge Zhang, Quy Duc Do, Xiang Yue, and Wenhui Chen. Long-context LLMs Struggle with Long In-context Learning, 2024.
- [9] Ramakrishna Bairi, Atharv Sonwane, Aditya Kanade, DC Vageesh, Arun Iyer, Suresh Parthasarathy, Sriram Rajamani, B Ashok, and Shashank Shet. Codeplan: Repository-level coding using llms and planning. 2023.
- [10] Nelson F Liu, Kevin Lin, John Hewitt, Ashwin Paranjape, Michele Bevilacqua, Fabio Petroni, and Percy Liang. Lost in the middle: How language models use long contexts. *Transactions of the Association for Computational Linguistics*, 12:157–173, 2024.
- [11] Jiaqi Li, Mengmeng Wang, Zilong Zheng, and Muhan Zhang. LooGLE: Can Long-Context Language Models Understand Long Contexts?, 2023.

[12] Freda Shi, Xinyun Chen, Kanishka Misra, Nathan Scales, David Dohan, Ed Chi, Nathanael Schärli, and Denny Zhou. Large language models can be easily distracted by irrelevant context, 2023.

[13] Ruixiang Tang, Dehan Kong, Longtao Huang, and Hui Xue. Large language models can be lazy learners: Analyze shortcuts in in-context learning. In *Findings of the Association for Computational Linguistics: ACL 2023*, pages 4645–4657, 2023.

[14] He Junqing, Pan Kunhao, Dong Xiaoqun, Song Zhuoyang, Liu Yibo, Liang Yuxin, Wang Hao, Sun Qianguo, Zhang Songxin, Xie Zejian, et al. Never lost in the middle: Improving large language models via attention strengthening question answering. *ArXiv preprint*, abs/2311.09198, 2023.

[15] Zhenyu Zhang, Runjin Chen, Shiwei Liu, Zhewei Yao, Olatunji Ruwase, Beidi Chen, Xiaoxia Wu, and Zhangyang Wang. Found in the Middle: How Language Models Use Long Contexts Better via Plug-and-Play Positional Encoding, 2024.

[16] Greg Kamradt. Needle in a haystack - pressure testing llms, 2023.

[17] Jun Zhao, Can Zu, Hao Xu, Yi Lu, Wei He, Yiwen Ding, Tao Gui, Qi Zhang, and Xuanjing Huang. Longagent: Scaling language models to 128k context through multi-agent collaboration. *ArXiv preprint*, abs/2402.11550, 2024.

[18] Yijiong Yu. Training With "Paraphrasing the Original Text" Improves Long-Context Performance, 2023.

[19] Shengnan An, Zexiong Ma, Zeqi Lin, Nanning Zheng, and Jian-Guang Lou. Make Your LLM Fully Utilize the Context, 2024.

[20] Yuhan Chen, Ang Lv, Ting-En Lin, Changyu Chen, Yuchuan Wu, Fei Huang, Yongbin Li, and Rui Yan. Fortify the Shortest Stave in Attention: Enhancing Context Awareness of Large Language Models for Effective Tool Use, 2023.

[21] Jianlin Su, Murtadha Ahmed, Yu Lu, Shengfeng Pan, Wen Bo, and Yunfeng Liu. Roformer: Enhanced transformer with rotary position embedding, 2024.

[22] Ofir Press, Noah A. Smith, and Mike Lewis. Train short, test long: Attention with linear biases enables input length extrapolation. In *The Tenth International Conference on Learning Representations, ICLR 2022, Virtual Event, April 25-29, 2022*. OpenReview.net, 2022.

[23] Adi Haviv, Ori Ram, Ofir Press, Peter Izsak, and Omer Levy. Transformer language models without positional encodings still learn positional information. In *Findings of the Association for Computational Linguistics: EMNLP 2022*, pages 1382–1390, Abu Dhabi, United Arab Emirates, 2022. Association for Computational Linguistics.

[24] Tri Dao. Flashattention-2: Faster attention with better parallelism and work partitioning. 2023.

[25] Hugo Touvron, Louis Martin, Kevin Stone, Peter Albert, Amjad Almahairi, Yasmine Babaei, Nikolay Bashlykov, Soumya Batra, Prajjwal Bhargava, Shruti Bhosale, et al. Llama 2: Open foundation and fine-tuned chat models. *ArXiv preprint*, abs/2307.09288, 2023.

[26] Wei-Lin Chiang, Zhuohan Li, Zi Lin, Ying Sheng, Zhanghao Wu, Hao Zhang, Lianmin Zheng, Siyuan Zhuang, Yonghao Zhuang, Joseph E. Gonzalez, Ion Stoica, and Eric P. Xing. Vicuna: An open-source chatbot impressing gpt-4 with 90%* chatgpt quality, 2023.

[27] Albert Q Jiang, Alexandre Sablayrolles, Arthur Mensch, Chris Bamford, Devendra Singh Chaplot, Diego de las Casas, Florian Bressand, Gianna Lengyel, Guillaume Lample, Lucile Saulnier, et al. Mistral 7b. *ArXiv preprint*, abs/2310.06825, 2023.

[28] Gemma Team, Thomas Mesnard, Cassidy Hardin, Robert Dadashi, Surya Bhupatiraju, Shreya Pathak, Laurent Sifre, Morgane Rivièvre, Mihir Sanjay Kale, Juliette Love, et al. Gemma: Open models based on gemini research and technology. *ArXiv preprint*, abs/2403.08295, 2024.

[29] Jinze Bai, Shuai Bai, Yunfei Chu, Zeyu Cui, Kai Dang, Xiaodong Deng, Yang Fan, Wenbin Ge, Yu Han, Fei Huang, Binyuan Hui, Luo Ji, Mei Li, Junyang Lin, Runji Lin, Dayiheng Liu, Gao Liu, Chengqiang Lu, Keming Lu, Jianxin Ma, Rui Men, Xingzhang Ren, Xuancheng Ren, Chuanqi Tan, Sinan Tan, Jianhong Tu, Peng Wang, Shijie Wang, Wei Wang, Shengguang Wu, Benfeng Xu, Jin Xu, An Yang, Hao Yang, Jian Yang, Shusheng Yang, Yang Yao, Bowen Yu, Hongyi Yuan, Zheng Yuan, Jianwei Zhang, Xingxuan Zhang, Yichang Zhang, Zhenru Zhang, Chang Zhou, Jingren Zhou, Xiaohuan Zhou, and Tianhang Zhu. Qwen technical report. *ArXiv preprint*, abs/2309.16609, 2023.

[30] MosaicML NLP Team. Introducing mpt-30b: Raising the bar for open-source foundation models, 2023. Accessed: 2023-06-22.

[31] Yushi Bai, Xin Lv, Jiajie Zhang, Hongchang Lyu, Jiankai Tang, Zhidian Huang, Zhengxiao Du, Xiao Liu, Aohan Zeng, Lei Hou, Yuxiao Dong, Jie Tang, and Juanzi Li. Longbench: A bilingual, multitask benchmark for long context understanding. *ArXiv preprint*, abs/2308.14508, 2023.

[32] Jie Wang, Tao Ji, Yuanbin Wu, Hang Yan, Tao Gui, Qi Zhang, Xuanjing Huang, and Xiaoling Wang. Length Generalization of Causal Transformers without Position Encoding, 2024.

[33] Ta-Chung Chi, Ting-Han Fan, Li-Wei Chen, Alexander Rudnicky, and Peter Ramadge. Latent positional information is in the self-attention variance of transformer language models without positional embeddings. In *Proceedings of the 61st Annual Meeting of the Association for Computational Linguistics (Volume 2: Short Papers)*, pages 1183–1193, 2023.

[34] Shouyuan Chen, Sherman Wong, Liangjian Chen, and Yuandong Tian. Extending Context Window of Large Language Models via Positional Interpolation, 2023.

[35] Erik Nijkamp, Tian Xie, Hiroaki Hayashi, Bo Pang, Congying Xia, Chen Xing, Jesse Vig, Semih Yavuz, Philippe Laban, Ben Krause, Senthil Purushwarkam, Tong Niu, Wojciech Kryściński, Lidiya Murakhovs'ka, Prafulla Kumar Choubey, Alex Fabbri, Ye Liu, Rui Meng, Lifu Tu, Meghana Bhat, Chien-Sheng Wu, Silvio Savarese, Yingbo Zhou, Shafiq Joty, and Caiming Xiong. Xgen-7b technical report. *ArXiv preprint*, abs/2309.03450, 2023.

[36] Yao Fu, Rameswar Panda, Xinyao Niu, Xiang Yue, Hannaneh Hajishirzi, Yoon Kim, and Hao Peng. Data engineering for scaling language models to 128k context. *ArXiv preprint*, abs/2402.10171, 2024.

[37] Bowen Peng, Jeffrey Quesnelle, Honglu Fan, and Enrico Shippole. Yarn: Efficient context window extension of large language models, 2023.

[38] Yiran Ding, Li Lyra Zhang, Chengruidong Zhang, Yuanyuan Xu, Ning Shang, Jiahang Xu, Fan Yang, and Mao Yang. LongRoPE: Extending LLM Context Window Beyond 2 Million Tokens, 2024.

[39] Amanda Bertsch, Uri Alon, Graham Neubig, and Matthew R. Gormley. Unlimiformer: Long-range transformers with unlimited length input. In *Thirty-seventh Conference on Neural Information Processing Systems*, 2023.

[40] Szymon Tworkowski, Konrad Staniszewski, Mikołaj Pacek, Yuhuai Wu, Henryk Michalewski, and Piotr Miłoś. Focused transformer: Contrastive training for context scaling. In *Thirty-seventh Conference on Neural Information Processing Systems*, 2023.

[41] Hao Liu, Matei Zaharia, and Pieter Abbeel. Ring attention with blockwise transformers for near-infinite context. 2023.

[42] Zhiyuan He, Huiqiang Jiang, Zilong Wang, Yuqing Yang, Luna Qiu, and Lili Qiu. Position engineering: Boosting large language models through positional information manipulation. *arXiv preprint arXiv:2404.11216*, 2024.

[43] Yifei Gao, Lei Wang, Jun Fang, Longhua Hu, and Jun Cheng. Empower Your Model with Longer and Better Context Comprehension, 2023.

- [44] Qingyu Yin, Xuzheng He, Xiang Zhuang, Yu Zhao, Jianhua Yao, Xiaoyu Shen, and Qiang Zhang. StableMask: Refining Causal Masking in Decoder-only Transformer, 2024.
- [45] Huiqiang Jiang, Qianhui Wu, Xufang Luo, Dongsheng Li, Chin-Yew Lin, Yuqing Yang, and Lili Qiu. LongLLMLingua: Accelerating and Enhancing LLMs in Long Context Scenarios via Prompt Compression, 2023.
- [46] Alexander Peysakhovich and Adam Lerer. Attention Sorting Combats Recency Bias In Long Context Language Models, 2023.
- [47] Wenhao Wu, Yizhong Wang, Guangxuan Xiao, Hao Peng, and Yao Fu. Retrieval Head Mechanistically Explains Long-Context Factuality, 2024.
- [48] Mingjie Sun, Xinlei Chen, J. Zico Kolter, and Zhuang Liu. Massive Activations in Large Language Models, 2024.

A Limitations

For different LLMs, an additional search cost is required to determine the positional hidden states including identify top-K positional hidden and evaluate on the small size validation dataset, which takes approximately 10 minutes for 7B level LLMs on a single A100 GPU.

Due to the difficulty in fully explaining the impact of some dimension to LLM’s behavior, the top-1 dimension returned by the searching algorithm may have the optimal performance on various tasks. Sometimes the optimal dimension is in the top-3 results.

Because of the recalculation of the query and key states, the additional time cost will increase linearly with the length of the input sequence.

B Broader Impacts

Our methods explore the intrinsic causes of position bias in LLMs and propose a way to alleviate this bias by pruning positional hidden states. This improves the inference capabilities of LLMs, making them more applicable to a wider range of scenarios, especially long-context LLMs and more complex applications. Additionally, our work promotes further research on the deep relationships between the causal mask, hidden states, attention weights and position bias in LLMs, aiding in the iterative development of related technologies.

C Experiment Details

C.1 Datasets Details

We choose NaturalQuestion Multi-document QA and Key-Value Retrieval datasets used in "lost in the middle" paper [10] to evaluate the degree to which our method alleviates position bias. NaturalQuestion Multi-document QA require the model to answer the question based on one key information document which is inserted in a long context consisting of many irrelevant documents. And Key-Value Retrieval needs the model to retrieve the value corresponding to the given key from a list consisting of hundreds of Key-Value pairs. These two datasets are both classic in-context tasks which aim to evaluate the differences of model performance when key information is located at different positions in the context. The evaluation metric is accuracy, based on whether the model’s response contains a string of the correct answer. In addition, we evaluate our method’s improvements across multi task types, using LongBench [31], a benchmark for bilingual, multitask, and comprehensive assessment of long context understanding capabilities of LLMs. It contains six major categories, covering single-document QA, multi-document QA, summarization, few-shot learning, synthetic tasks and code completion. The evaluation metrics are: F1 for single-document QA and multi-document QA, Rouge-L for summarization, accuracy (exact match) for few-shot learning and synthetic tasks, and edit similarity for code completion. During inference, since the original context may sometimes be too long, the input sequences will be truncated in the middle part to avoid exceeding the context window of the model.

C.2 Additional Implementation Details

Curve Fitting When we perform curve fitting on $h(p)$, we use least-squares cubic polynomial fit. And when judging its monotonicity, we skip the first 100 positions because the first a few values are often outliers. Since $h(p)$ is originally a discrete function, in practice, we employ the second-order difference to approximate the second-order derivative when computing smoothness.

Ms-PoE on Mistral When applying Ms-PoE [15] to mistral-7b [27] with its default parameters (minimal scale factor is 1.2 and maximal is 1.8), we found the model fail to generate normal responses, so we set the maximal scale factor to 1.2, under which Ms-PoE [15] is equal to PI [34] with scale factor 1.2.

Ablation of the Searching Algorithm We conducted ablation experiments to demonstrate the necessity of using the three indicators (monotonicity, smoothness, validation loss) in our searching algorithm. Ours w/o monotonicity means we just select top-10 smoothest dimensions and then use

the validation loss to determine. Ours w/o smoothness means we select top-10 dimensions with the highest number of monotonic layers and then use validation loss. Ours w/o validation loss means we first select top-10 dimensions with the highest number of monotonic layers and then just choose the smoothest one among them.

C.3 Scaled Dimensions Details

Table 4: The scaled dimensions, scale factors and applied layers of models.

Model	Dimension	Scale factor	Applied layers
LLaMA-2-7b-chat	2,393	-1	10~25
LLaMA-2-13b-chat	4,283	-1	10~34
Vicuna-7b-v1.5-16k	2,393	0	10~25
Vicuna-13b-v1.5-16k	4,923	0	10~34
Mistral-7B-Instruct-v0.2	213	0	10~25
Gemma-1.1-7b-it	1,665	0	10~22
Qwen1.5-7b-chat	1,081	0.2	10~25
MPT-30b-chat	6,926	0	10~42

The scaled dimensions, scale factors and applied layers of each model we use in our experiments are shown in Table 4.

C.4 Inference Latency

Table 5: Time consumed (minutes) of LLaMA-2-7b-chat in a single A100.

Method	KV Retrieval	NaturalQuestion
FlashAttention-2	22	14
Ours	32	15
Ms-PoE	61	26

Table 5 shows the running time of LLaMA-2-7b-chat with different methods in the KV retrieval dataset consisting of 500 samples with average length of about 10,000, and the multi-document QA dataset consisting of 500 samples with average length of about 3,300. Our method requires recompute the query and key states, thus inevitably requires more time compared to baseline, but the cost is within an acceptable range. In contrast, Ms-PoE [15] need to compute the attention weights twice, resulting in a doubling of time consumption.

D Obtain Attention to Key Information

To avoid the influence of internal knowledge in the model and make attention calculation simpler, we conduct a KV retrieval task, whose prompt format is as follows:

Json data: {"os08jkb1limft6wgxeda": "imx6lyp4b8ogjaq7ret1",(n key-value pairs)} The value of key "os08jkb1limft6wgxeda" is "

The last token of the prompt will directly take on the task of predicting the answer, i.e., the value which need to be retrieved. Hence, the last token's attention weights to the previous text can reflect whether it accurately retrieves the key information. We define the model's attention (in some layer) to the key information as A_G in Eq 6, where G represents the set of token positions corresponding to where the key information is at, l is the position of the last token of the prompt, and $a_{l,j}$ represents the attention weight of the l -th token to the j -th token. By shifting G , we use the same method to calculate its attention to each other KV pairs.

$$A_G = \frac{1}{|G|} \sum_{j \in G} a_{l,j} \quad (6)$$

E Attention v.s. Performance

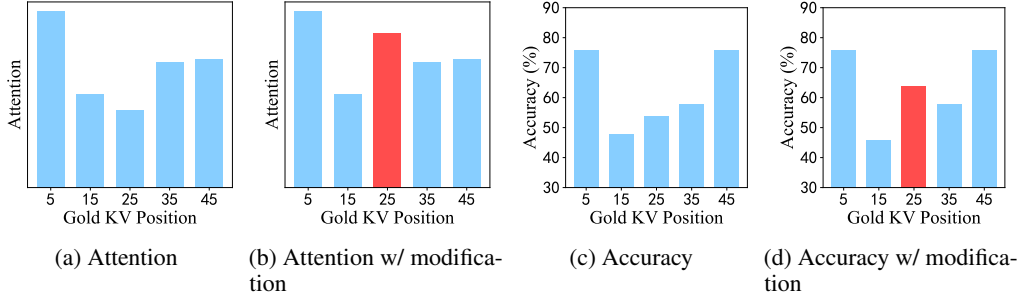


Figure 6: Distribution of attention weight and accuracy as the ground-truth KV is placed at different positions in the prompt. (b) and (d) are situations when the attention on the 25th KV pair is modified.

As illustrated in Figure 6, when we manually multiply all the attention weights to the tokens belong to the key information (here we only choose the 25th KV pair, as shown in Figure 6b) by 2 in the model’s forward process on the KV retrieval task, the corresponding retrieval accuracy of the 25th KV also show improvements, while the other parts mainly keep unchanged, as shown in Figure 6d. This result proves that the attention weights for the key information is positively correlated with the retrieval accuracy.

F How We Modify Causal Mask and Position Embedding in KV Retrieval

In the method 1 in section 2.2, we crop the causal mask to let the "key tokens" unable to attend the previous tokens. As shown in Figure 7, the white part represents the cropped part, which means attention weights are 0, and the orange part represents the attention between tokens within key tokens. In addition, we have retained the attention of key tokens to the first token to maintain the stability of attention distribution. What is more, we only modify the causal mask in layers 1~8, but as the results, the attention to the key information is still significantly improved in layers 15~31, which indicates the positional information generated by causal mask in former layers can be transmitted to latter layers using posisional hidden states as the medium, thus modifying the causal mask solely in the former layers can induce a profound shift in the model’s comprehension of positional information.

In the method 2 and 3 in section 2.2, we modify the position embeddings through altering the position ids. The specific operation is shown in the Figure 8, in which we directly replace the position ids corresponding to the key tokens with the position ids of the starting tokens (or the ending tokens), and actually only the attention weights of the last token to previous tokens are modified. We apply this modification in all the layers. Compared to modifying the causal mask, if only modify position embedding in former layers, the attention in the latter layers remains almost unchanged, which indicates the positional information generated by position embedding may be temporary and can hardly be transmitted across layers.

G Perturbation on Causal Mask and Position Embedding

To further explore the origin of these position hidden states, we performed perturbation experiments. As depicted in Figure 9c, subtracting 200 from the position ids corresponding to the 400th to 600th tokens (reducing PE) had only a minor effect on the position hidden states, whereas, in Figure 9b, crop the causal mask to make the 400th to 600th tokens unable to attend the 1st to 400th tokens (cropping causal mask) led to significant fluctuations in positional hidden states of the 400th to 600th tokens. This result proves the causal mask is the main factor causing this kind of positional hidden states, and it is the token’s position in the causal mask that determines its value in the positional hidden states, but not position ids of position embedding.

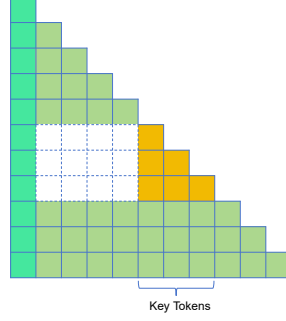


Figure 7: Cropping the causal mask to let key tokens unable to see previous tokens, except the first token.

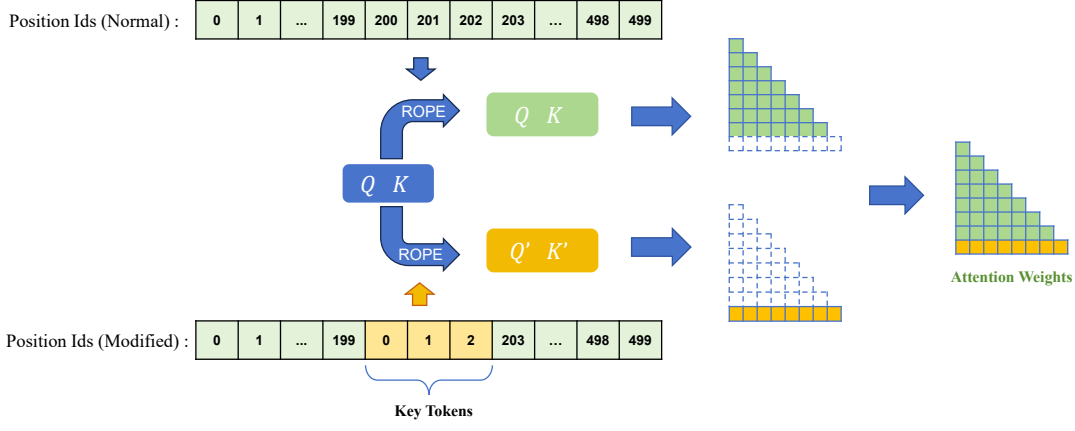


Figure 8: Shifting position ids to the start (PE to beginning).

H Does this Method Compromise the Ability to Perceive Positional Information?

To prove our method is harmless for position-sensitive tasks though eliminating some positional information, we conduct the timeline reorder task from LooGLE [11], whose objective is to arrange the events in accordance with their chronological sequence as dispersed throughout the extensive text. The results in Table 6 proved our methods will not impair model’s performance on position-sensitive tasks. This also reflects that the positional information we eliminate may not be necessary for the model to function well.

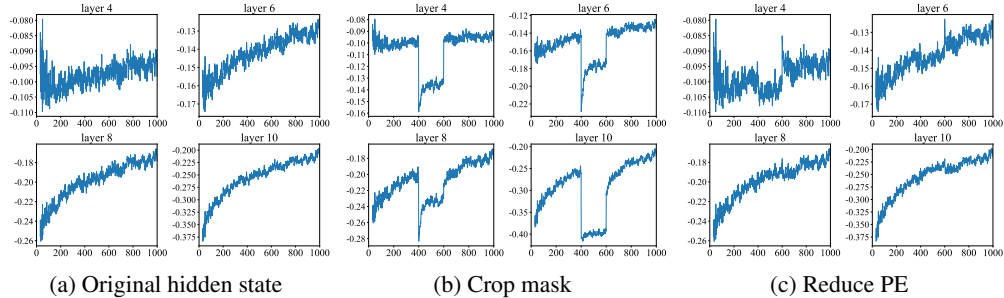


Figure 9: We performed perturbation experiments on the causal mask and position embedding (PE), showing the dimension 213 of hidden states of Mistral-7b [27] using randomly synthesized corpus as input.

Table 6: Performance of difference models on position-sensitive task-timeline reorder [11].

Model	Accuracy
Vicuna-7b-v1.5-16k	20.83
Vicuna-7b-v1.5-16k w/ Ours	20.83
Qwen1.5-7b-chat	28.13
Qwen1.5-7b-chat w/ Ours	28.13
Mistral-7B-Instruct-v0.2	18.75
Mistral-7B-Instruct-v0.2 w/ Ours	19.79

I Attention Distribution Layer-wise and Head-wise

Figure 10 shows Mistral-7b’s attention to each KV pair of each layer (average across all attention heads) in the context in a KV retrieval task when the gold KV is put at different positions. The y-axis is the gold KV’s position, x-axis is each KV’s position, and the scale of the colorbar represents attention (10^{-3}). We can observe that diagonal patterns, which indicates the attention is concentrated on the “key tokens”, appear only in the latter layers (start from layer 14), and may be a manifestation of retrieval behavior. In contrast, the former layers only focus on the beginning or end, regardless of where the key information is located.

Figure 11 shows the head-wise situation of layer 15. We can see actually only a portion of attention heads exhibit diagonal patterns, which may correspond to *retrieval heads* [47]. The attention distribution in these heads also shows a pattern corresponding “loss in the middle”, being larger at the beginning or end while significantly smaller at the middle.

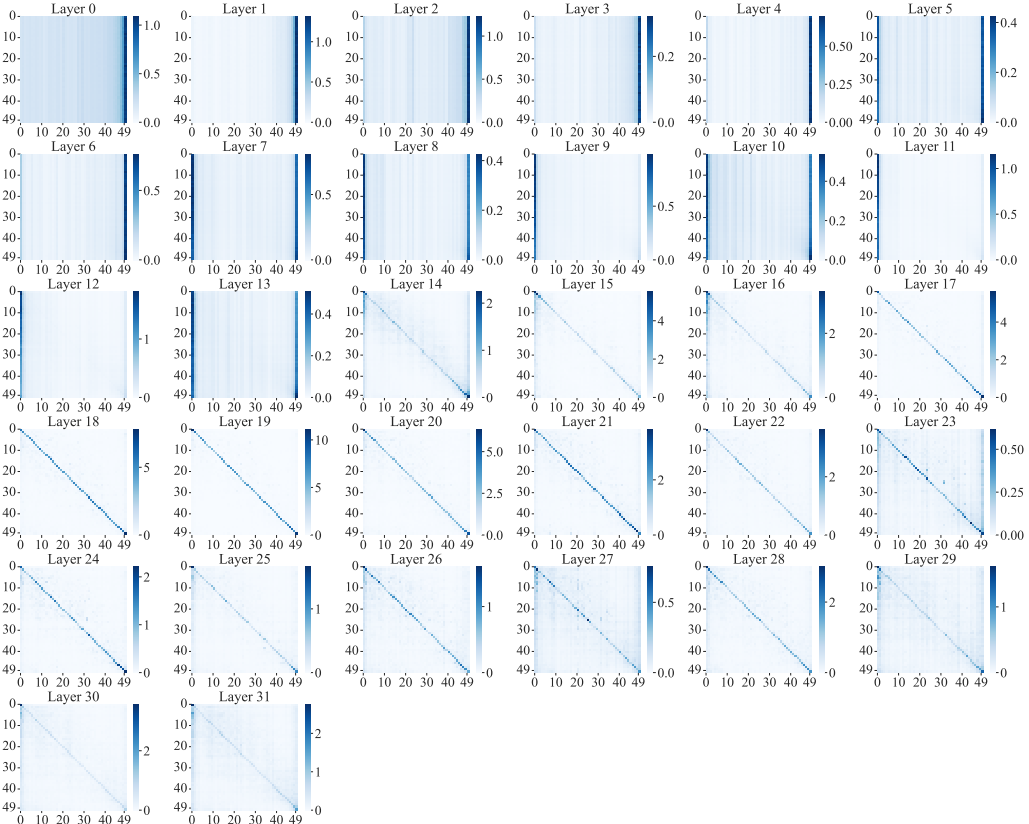


Figure 10: The average attention weight distributed on each KV, of all the 32 layers of Mistral-7b, on a 50 KV pairs retrieval task, when the gold KV is put at each different position.

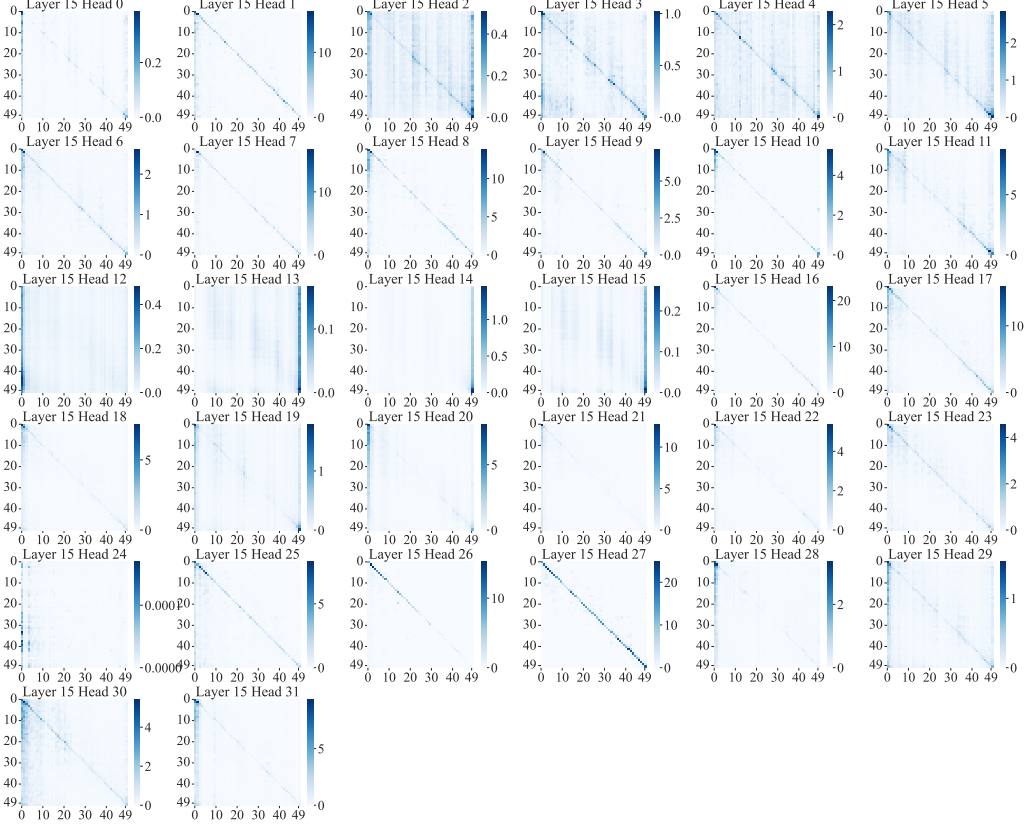


Figure 11: The average attention weight distributed on each KV, of all the 32 attention heads of layer 15 of Mistral-7b, on a 50 KV pairs retrieval task, when the gold KV is put at each different position.

J Positional Hidden States Visualization

We show various models’ positional hidden states of each layer in Figure 12. When visualizing, we discarded the first 30 tokens because the hidden states values of these tokens are often huge (usually hundreds of times larger than the normal value [48]), which can disrupt monotonicity. We observed its monotonic trend first appears just in the first layer (actually just after the first attention mechanism), and continue to be more marked.

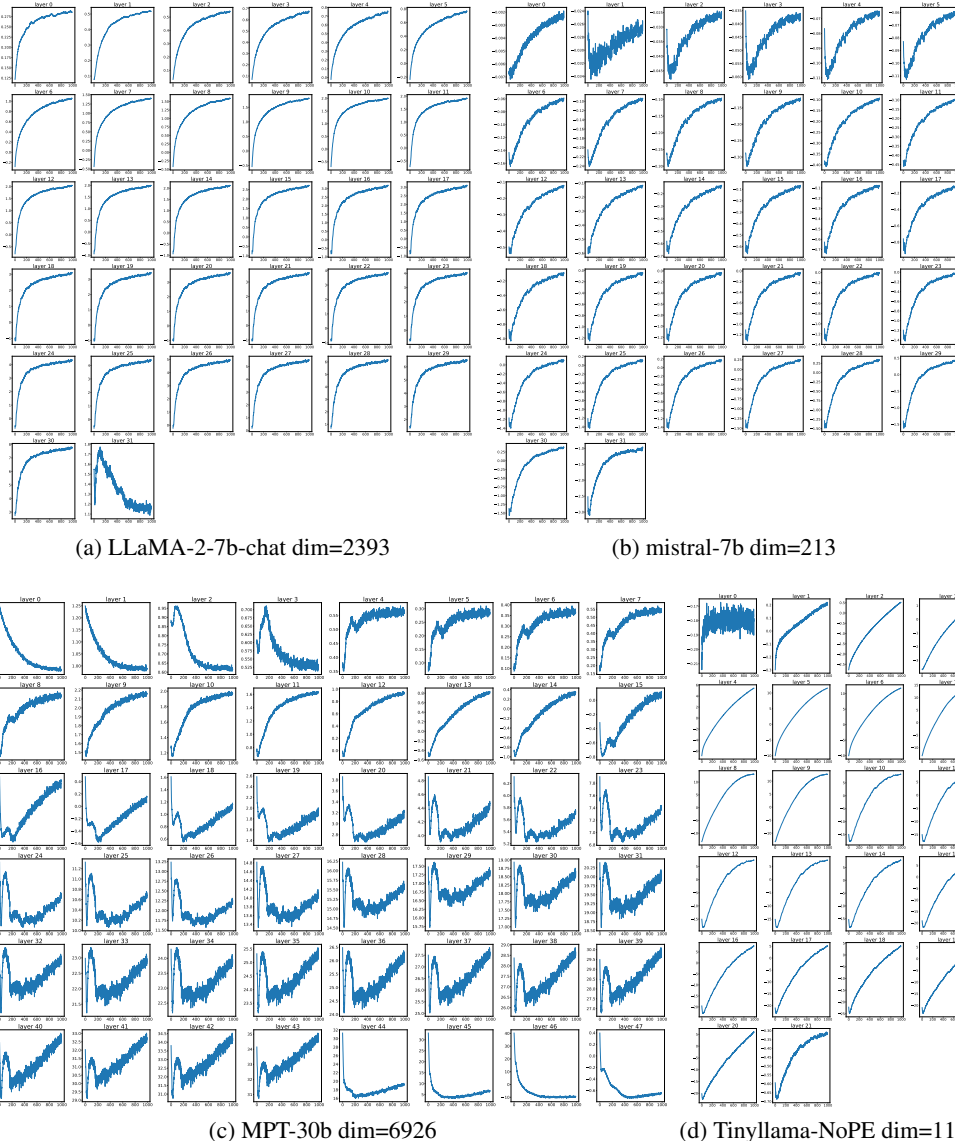


Figure 12: Positional hidden states output by each layer of LLaMA-2-7b-chat, Mistral-7b-Instruct-v0.2, MPT-30b-chat and TinyLlama-NoPE-1.1B. The x-axis represents the position, and the y-axis represents the value of the states.